

# Path loss of non-line-of-sight ultraviolet light communication channel in polydisperse aerosol systems\*

MA Yuzhao<sup>1,2\*\*</sup>, JIA Huiting<sup>2</sup>, GAO Huiliang<sup>2</sup>, and XIONG Xinglong<sup>1,2</sup>

1. Tianjin Key Laboratory for Advanced Signal Processing, Civil Aviation University of China, Tianjin 300300, China

2. College of Electronic Information and Automation, Civil Aviation University of China, Tianjin 300300, China

(Received 24 July 2021; Revised 1 October 2021)

©Tianjin University of Technology 2022

Performance of non-line-of-sight (NLOS) ultraviolet (UV) communication is closely related with the system geometry, the communication range, and the atmospheric parameters. In this paper, we implement a full numerical analysis of the relations of path loss of NLOS UV communication with these factors using the Mie scattering theory and the Monte-Carlo method. In the numerical simulations, the actual polydisperse aerosol systems are used as the transmission medium. Since for the actual aerosol systems the atmosphere conditions may be similar within a short period, the path loss may be exclusively determined by the atmosphere visibility. Hence, we build a relation between the path loss of the communication channel and the atmosphere visibility. Simulation results reveal that for a relatively small communication range, the path loss increases with the visibility. On the other hand, low elevation of the transceiver may reduce the path loss. Our simulation results are useful for the evaluation of performance of the real NLOS UV communication systems.

**Document code:** A **Article ID:** 1673-1905(2022)03-0158-8

**DOI** <https://doi.org/10.1007/s11801-022-1122-x>

The ozone sphere of the atmosphere may strongly absorb the ultraviolet (UV) light of 20—280 nm within the solar radiation, i.e., in the lower atmosphere there is almost no solar radiation of the waveband. Therefore, the UV light with the wavelength smaller than 280 nm is regarded as solar-blind. In this context, the UV light communication seems to be promising for it can be built without considering the background noise produced by the solar radiation and may operate simultaneously with the existing radio frequency systems. With the development of the novel photonic devices, non-line-of-sight (NLOS) UV light communication systems have drawn special attentions<sup>[1-19]</sup>.

An NLOS UV communication system is a bistatic system with the transmitter and the receiver being located in different places. The receiver of the NLOS UV communication system measures the scattering of the light. An NLOS UV communication system is interesting when the free-space communication is necessary and a line-of-sight (LOS) link cannot be built. GARG et al<sup>[7]</sup> derived the average symbol error rate of NLOS UV communications in turbulent atmosphere for quadrature amplitude modulation (QAM) schemes. SONG et al<sup>[8]</sup> studied the pulse response characteristics of the NLOS UV single-scatter communication in mobile scene. Path loss of the communication channel is the most important factor that determines the communication performance. A great deal of work in path loss of NLOS UV commu-

nication channels was reported<sup>[9-16]</sup>. CAO et al<sup>[9]</sup> proposed a Monte-Carlo model for calculating the single-scatter path loss of NLOS UV communication channels, considering the Lambertian distribution of the light emitting diode (LED) source emission. DING<sup>[10]</sup> and XU<sup>[11]</sup> have modeled the path loss of NLOS UV channels for different wavelengths. XU et al<sup>[11]</sup> used the wide-spectra Mie phase function for discussions on the path loss and the data rate of NLOS UV channels. ZHANG et al<sup>[12]</sup> have studied the polarization characteristics in NLOS UV communication channels based on a vectorized polarization-sensitive model of NLOS multiple-scatter propagation. DROST et al<sup>[13]</sup> demonstrated the path loss of the NLOS UV communication channels with different orders of scattering being considered. However, in these investigations, specific atmosphere parameters, e.g., aerosol extinction coefficient and asymmetry factor, were assumed. The effects of atmosphere condition on the path loss of the NLOS UV communication channels have been studied in Refs.[14—16]. XU et al<sup>[14]</sup> studied the effects of the aerosol density and the radius on the path loss of the communication channels. DING et al<sup>[15]</sup> predicted the path loss for tenuous, thick, and extra thick atmosphere by assuming different extinction coefficients of the atmosphere. LIN et al<sup>[16]</sup> included the two types of fog in his research on the path loss of NLOS UV channels. Nevertheless, so far the

\* This work has been supported in part by the National Natural Science Foundation of China (No.U1833111).

\*\* E-mail: yzma@cauc.edu.cn

microphysical characteristics, e.g., particle size distribution and complex refractive index of the particles, in the actual polydisperse aerosol systems have not been considered in predicting the path loss of the NLOS UV communication channels. On the other hand, atmosphere visibility is an important macroscopic quantity of atmosphere closely related with the aerosol microphysical characteristics. A relation between the path loss of the communication channel and the atmosphere visibility would be interesting.

In the present work, we investigate the path losses of the NLOS UV communication channels with respect to the system geometry, communication range, and the atmospheric parameters. The considered polydisperse aerosols are aerosol systems possessing the lognormal particle size distributions and the actual aerosols. The relation between the path loss of the channel and the atmosphere visibility is demonstrated.

Assume the number density of the particles is  $N$ . The particle size distribution is defined by the number of the particles within the unit radius interval per unit volume as

$$n(r) = \frac{dN}{dr}. \tag{1}$$

Considering polydisperse aerosol of single composition suspending close to the ground, the particle size distribution of the aerosols can be expressed by a lognormal function as

$$n(r) = \frac{C}{r\sqrt{2\pi} \ln \sigma} \exp\left[-\frac{\log^2(r/r_m)}{2\log^2 \sigma}\right], \tag{2}$$

where  $C$  is a constant dependent on the particle density,  $r_m$  is the mean radius, and  $\sigma$  is the standard derivation.  $n(r)$  and the complex refractive indices  $m$  are shown in Tab.1 for water-soluble and non-water-soluble aerosols<sup>[20]</sup>. Sometimes the volume logarithmic particle size distribution is also used:

$$\frac{dV}{d \ln r} = \frac{4\pi r^4}{3} n(r). \tag{3}$$

The actual atmosphere is the polydisperse aerosol system composed of a variety of aerosol compositions mixed with each other in different forms. The size distribution of the actual aerosols can be regarded as the superposition of several lognormal functions with different parameters.

**Tab.1 Parameters of two types of aerosols**

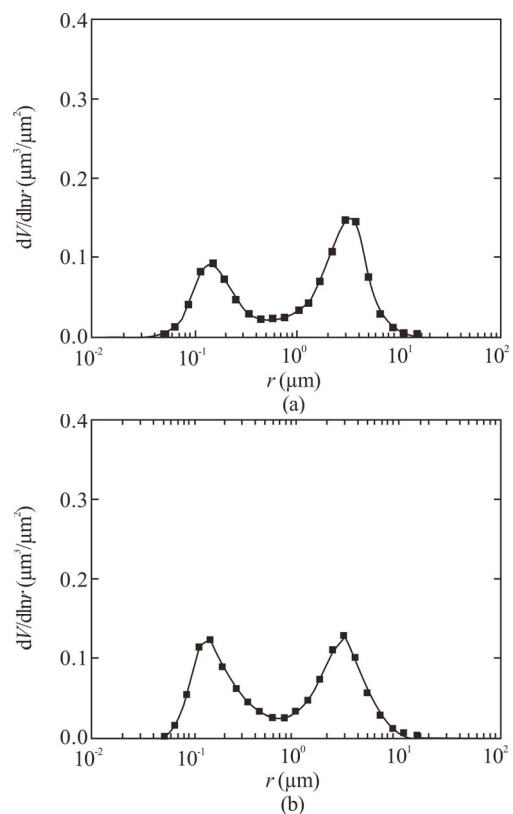
Aerosol type	$r_m$ ( $\mu\text{m}$ )	$\sigma$	$m$
Water soluble	0.021 2	2.24	1.45+0.015i
Non water soluble	0.471	2.51	1.50+0.030i

In this paper we intend to model the path loss of the NLOS UV communication in the actual polydisperse aerosol systems in low-visibility weather. Firstly, we look through the visibility of each day from Sep. 1, 2017 to Apr. 30, 2018 in Beijing, China in the website for worldwide weather report. Four days of low-visibility are concerned. The four days are within a short time horizon. Their atmosphere conditions are expected to be similar. We may be able to build a relation between the path loss of the communication channel and the atmosphere visibility.

However, offers visibility data with very low resolution in time and space (one value for visibility per day per city). Secondly, we find the size distributions and the complex refractive indices at the concrete times of the four days in AERONET<sup>[21]</sup>. The data of observation station, Beijing\_RADI, locating at 40.004 80° N and 116.378 60° E are used. The refractive indices of the aerosols at 250 nm, the typical wavelength for the UV light communication, are derived using the refractive indices of the aerosols at 440 nm, 670 nm, 870 nm, and 1 020 nm obtained in AERONET<sup>[21]</sup>, shown in Tab.2. The calculated standard visibilities are also illustrated in the table. The basic equations for the standard visibility calculation will be detailed later. It is seen that in the table the visibilities on Feb. 26 and Mar. 3 are around 5 km and the visibilities on Mar. 13 and Mar. 14 are around 3 km. According to the criterion for the visibility levels issued by the world meteorological organization (WMO), the atmosphere condition is light haze on Feb. 26 and Mar. 3, and haze on Mar. 13 and Mar. 14. The volume logarithmic particle size distributions of the polydisperse aerosol systems are shown in Fig.1. It is seen that the actual aerosol systems of the four days can be regarded as the superpositions of two lognormal size distribution functions with different densities.

**Tab.2 Refractive indices and standard visibilities of the actual aerosols**

Time (GMT)	$m$ (250 nm)	$V$ (km)
Feb. 26 00:20:49	1.499 0 + 0.010 9i	5.6
Mar. 3 00:41:02	1.490 2 + 0.008 0i	5.1
Mar. 13 07:26:35	1.627 6 + 0.010 5i	2.6
Mar. 14 04:26:12	1.421 0 + 0.004 9i	3.5



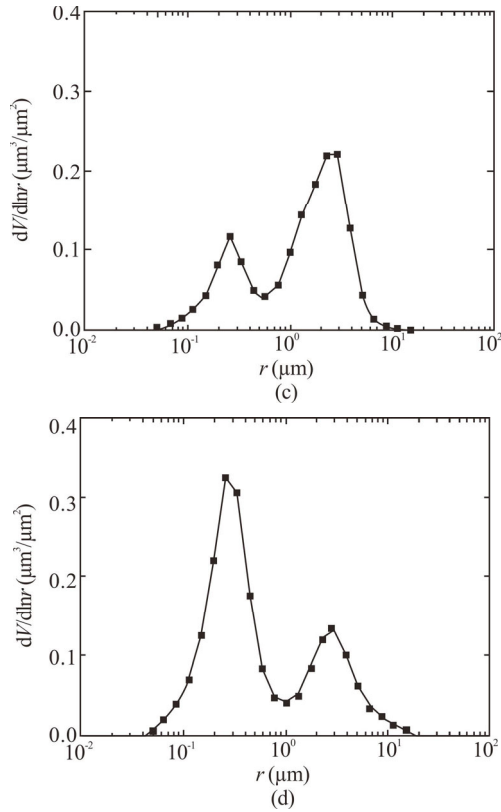


**Fig.1 Volume logarithmic particle size distributions of the polydisperse aerosol systems in the actual atmosphere: (a) Feb. 26; (b) Mar. 03; (c) Mar. 13; (d) Mar. 14**

The single scattering properties of aerosols are described by asymmetry factor  $g$ , scattering coefficient  $k_s$ , absorption coefficient  $k_a$ , and the extinction coefficient  $k_e$  with the relation  $k_e = k_s + k_a$ . In reality, the visibility, known as visual range, is often used to evaluate the quality of atmosphere. Following the Koschmieder's law, visibility can be deduced using the extinction coefficient as

$$V = -\frac{\ln \varepsilon}{k_e}, \quad (4)$$

where  $\varepsilon$  is the contrast threshold of the observer, and  $k_e$  is the extinction coefficient at 550 nm.  $\varepsilon=0.02$  is used for the standard visibility. The normalized asymmetry factor of the polydisperse aerosol system can be calculated as

$$g = \frac{\int_{r_{\min}}^{r_{\max}} g(r)n(r)C_{\text{ext}}(r)dr}{\int_{r_{\min}}^{r_{\max}} n(r)C_{\text{ext}}(r)dr}, \quad (5)$$

where  $g(r)$  is the asymmetry factor for specific particle radius and  $C_{\text{ext}}(r)$  is the extinction cross section for specific particle radius. The single scattering characteristics of the water-soluble and non-water-soluble aerosol systems are shown in Tab.3. The single scattering characteristics of the actual aerosol systems are derived, shown in Tab.4. The extinction coefficient, scattering coefficient, absorption coefficient, and the normalized asymmetry factor at 250 nm are shown. The extinction coefficient at 550 nm and the standard visibility are also shown. The measured

visibilities are also demonstrated in Tab.4. The visibilities were measured by the forward scatter meter DNQ1 made by China Huayun Group, maintained by the Beijing Meteorological Service. The single scattering characteristics shown in the tables are used in predicting the path loss of the NLOS UV communication channel.

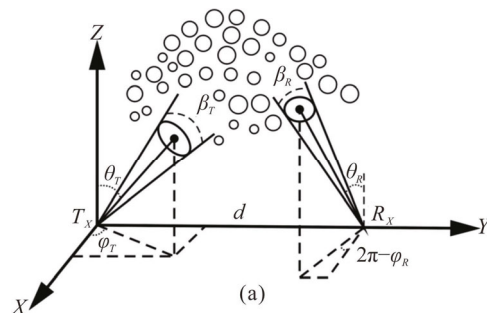
**Tab.3 Single scattering characteristics for typical polydisperse aerosol systems (coefficients are in  $\text{km}^{-1}$ , visibilities are in km)**

Aerosol type	$k_e$	$k_s$	$k_a$	$k_{e,550}$	$V$	$\bar{g}$
Water soluble	0.233 3	0.229 7	0.003 5	0.035 1	111.8	0.70
Non water soluble	1.913 2	1.316 1	0.597 2	1.999 1	2.0	0.88

**Tab.4 Single scattering characteristics for actual polydisperse aerosol systems (coefficients are in  $\text{km}^{-1}$ , visibilities are in km)**

Time	$k_e$	$k_s$	$k_a$	$k_{e,550}$	$V$	$V_m$	$\bar{g}$
Feb. 26	1.83	1.67	0.16	0.70	5.6	5.7	0.87
Mar. 03	2.39	2.23	0.15	0.76	5.1	5.5	0.87
Mar. 13	3.69	3.29	0.41	1.53	2.6	2.1	0.87
Mar. 14	3.40	3.28	0.18	1.11	3.5	3.0	0.86

The geometry of the considered NLOS UV communication channel is depicted in Fig.2. The transmitter locates at the origin of the coordinate system. As seen in Fig.2(a), the pointing direction of the transmitter is expressed by  $(\theta_T, \varphi_T)$ .  $\beta_T$  is the beam width of the transmitter. The directions of the emitted photons are determined by the pointing direction of the transmitter and the deflection angle given by the spatial distribution of the light source. The receiver has the distance of  $d$  from the transmitter. The pointing direction of the receiver is given by  $(\theta_R, \varphi_R)$ .  $\beta_R$  represents the field of view (FOV) of the receiver. The overall detection probabilities are determined by the system geometry, the communication range, and the atmospheric parameters. In order to obtain the desired detection probabilities, the pointing directions of the transmitter and receivers are normally set to in the same plane. In particular, both pointing directions are in the YOZ plane, seen in Fig.2(b). In the numerical simulations we use  $\varphi_T=90^\circ$  and  $\varphi_R=270^\circ$ .



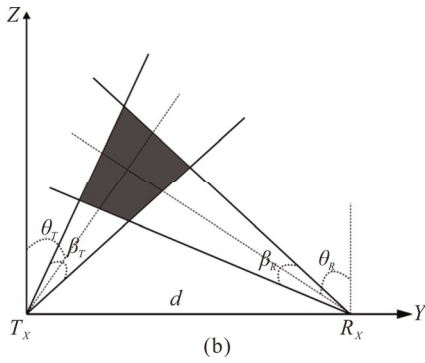


**Fig.2 Geometry of the NLOS UV communication channel: (a) Arbitrary transceiver arrangement; (b)  $\varphi_T=90^\circ$  and  $\varphi_R=270^\circ$**

The Monte-Carlo method used for modeling the path loss of the NLOS UV communication channel is detailed in Ref.[10]. Here we briefly state the process, as shown in Fig.3. Each scattering event may change the trajectory of the photon. The trajectory of the photon is determined by the direction cosine and the travelling distance before the photon reaches the next scatter. Assuming the travelling direction is given by the angle pair  $(\theta_s, \varphi_s)$  in the spherical coordinates via the scattering angle, determined by the generalized Henyey-Greenstein (HG) function as

$$P_{\text{Mie}}(\theta_s) = \frac{1-g^2}{4\pi} \left[ \frac{1}{(1+g^2-2g\cos\theta_s)^{3/2}} + \frac{3\cos^2\theta_s-1}{4(1+g^2)^{3/2}} \right]. \quad (6)$$

The normalized asymmetry factor, given by Eq.(5) is used for the polydisperse aerosol system. The azimuth angle of the scattered photon  $\theta_s$  is assumed to be uniformly distributed within  $[0, 2\pi]$ . The HG scattering phase function is well known for describing the scattering effects of light in atmosphere aerosols. Meanwhile, there are miscellaneous molecules as well in the atmosphere. Correspondingly, the Rayleigh scattering phase function is known for describing the scattering effects of light in atmosphere molecules. However, in the paper we study the path loss of NLOS UV light communication in the low atmosphere. We consider the interaction of the light with aerosols for aerosols are dominant in the low atmosphere. Therefore, only HG scattering phase function is relevant in this regime. Additionally, the travelling distance between the transmitter and the first scattering center or between two consecutive scattering centers is determined by

$$\Delta d = -\frac{1}{k_c} \ln \xi, \quad (7)$$

where  $\xi$  is a uniform random variable between 0 and 1. Only photons those impinge on the receiver within the FOV of the receiver contribute the detection probability. To ensure the photon to impinge on the receiver, i.e., the photon trajectory intercepts the receiver, three conditions have to be satisfied, shown in the dotted box in Fig.3. The extension line of the photon path has to intersect the receiver. The photon should travel toward the receiver and also far enough to the receiver. It is noted that only

the photon that is scattered but not absorbed by the aerosol may be captured by the receiver. Hence the probability of the photon being scattered is directly related with the ratio of the scattering coefficient to the extinction coefficient  $k_s/k_e$ . For non-absorb media  $k_s/k_e=1$ , while for aerosol with significant imaginary part of the complex refractive index, the absorption coefficient  $k_a$  cannot be ignored, and  $k_s/k_e < 1$ . Finally, after all photons of all scattering orders are traced, an estimate of the overall detection probability is given by the ratio of the sum of the photons' detection probabilities to the total number of simulated photons. The path loss of the NLOS UV communication channel is hence calculated.

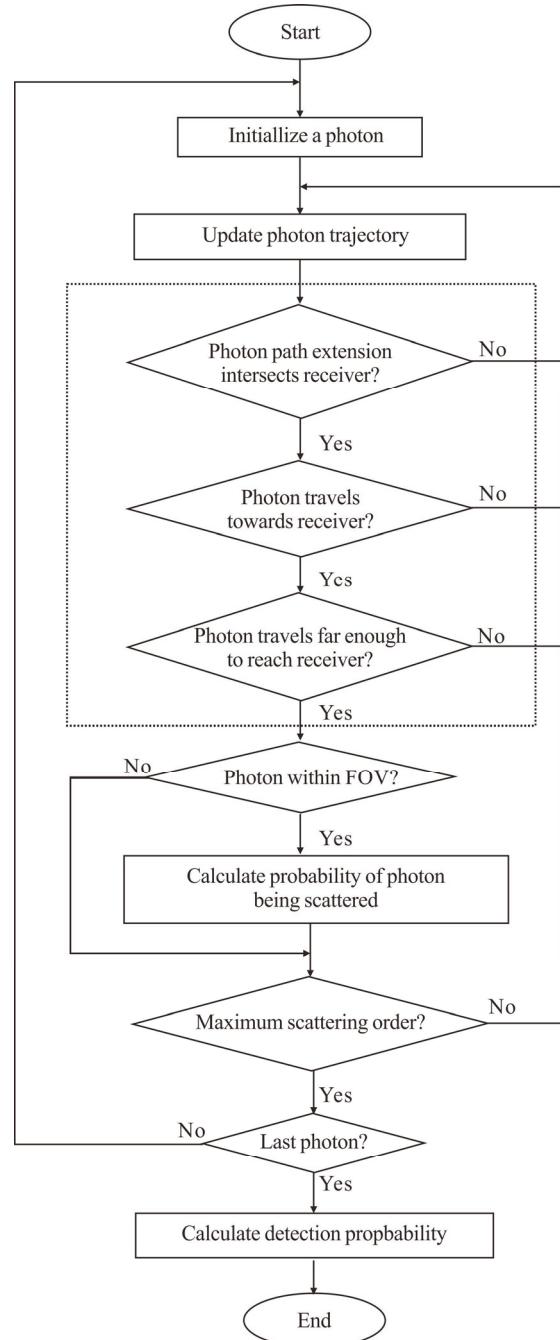


**Fig.3 Simulation path loss of the NLOS UV communication channel using Monte Carlo method**

We have numerically simulated the path loss of NLOS UV communication channel at 250 nm. The simulation parameters are shown in Tab.5, following Refs.[5,7]. In the numerical simulations of the path losses of the water-soluble, the non-water-soluble, and the actual polydisperse aerosol systems using the Monte-Carlo method<sup>[14-16]</sup>, the maximum scattering order is set to be 5. For a computer with Intel Core 3.2 GHz central processing unit (CPU), 12 GB memory, and 64 bit operation system, less than 1 h is needed for the photon number of  $10^{10}$ . The path losses were calculated for the communication range  $d=20\text{--}200$  m with the step of 20 m.

**Tab.5 Simulation parameters**

Parameter	Value
$\lambda$	250 nm
$\theta_T$	$30^\circ, 60^\circ$
$\theta_R$	$30^\circ, 60^\circ$
$\varphi_T$	$90^\circ$
$\varphi_R$	$270^\circ$
$\beta_T$	$10^\circ$
$\beta_R$	$30^\circ$
Receiver area	$1.77\text{ cm}^2$

Path losses of NLOS UV communication channel are demonstrated in Fig.4, considering the first order scattering, the high order scattering (the 2nd, 3rd, 4th and 5th order scattering), and all order scattering. The extinction coefficient  $k_e=3\text{ km}^{-1}$  and the asymmetry factor  $g=0.865$  are used. As expected, the path loss increases with respect to the communication range. Hence, the NLOS UV communication channel may operate with good performance only for limited communication range. It is noted that the difference of the path losses for the first order scattering and all order scattering can be as significant as several dBs. Furthermore, the difference increases via the communication range. Hence, the multiple-scattering effects cannot be ignored when the performance of the NLOS UV communication channel is to be studied.

We study the effects of the atmosphere condition on the path loss. The path losses are calculated for different aerosol extinction coefficients and the asymmetry factors for  $d=50$  m and  $d=200$  m, shown in Fig.5 and Fig.6. The path loss for small communication range ( $d=50$  m) is smaller than that for long communication ( $d=200$  m), as expected for all communication channels.  $g=0.865$  is used. It is seen in Fig.5 that the path loss is not sensitive to the extinction coefficient for relatively small extinction coefficient ( $k_e < 2.5\text{ km}^{-1}$ , relatively good weather). This is true for both  $d=50$  m and  $d=200$  m. However, for larger aerosol extinction coefficient ( $k_e > 2.5\text{ km}^{-1}$ , relatively bad weather), the variation tendencies of the path

loss are obviously different for  $d=50$  m and  $d=200$  m. For  $k_e > 2.5\text{ km}^{-1}$  and  $d=50$  m, the path loss decreases by  $k_e$ . For  $k_e > 2.5\text{ km}^{-1}$  and  $d=200$  m, the path loss increases by  $k_e$ . Hence, we may conclude that within a limited range, e.g.,  $d=50$  m, the performance of the NLOS UV communication may be better for bad weather than good weather. This can be the advantage of NLOS UV communication. In comparison, this situation will not remain for long communication range, e.g.,  $d=200$  m. In fact, the path loss also depends on the ratio of the scattering coefficient to the extinction coefficient  $k_s/k_e$ , which has been explained previously. The effects of the aerosol asymmetry factor on the path loss are shown in Fig.6, where  $k_e=1.5\text{ km}^{-1}$ . The variation tendencies of the path losses are similar for  $d=50$  m and  $d=200$  m. The path loss increases slowly by the asymmetry factor. Larger  $g$  means better ability of the scattering at the forward direction. Light is scattered less to the side. Hence, the receiver, which is installed at the same level to the transmitter, may capture less scattered light, resulting in larger path loss of the channel.

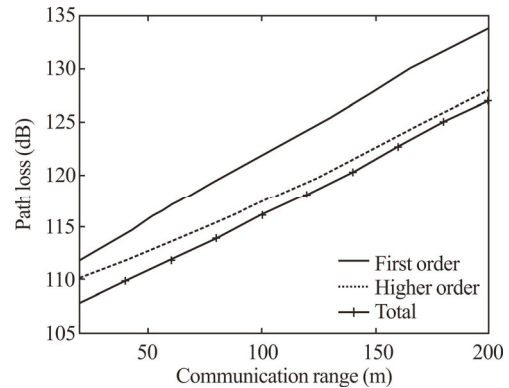


**Fig.4 Path losses for different orders of scattering**

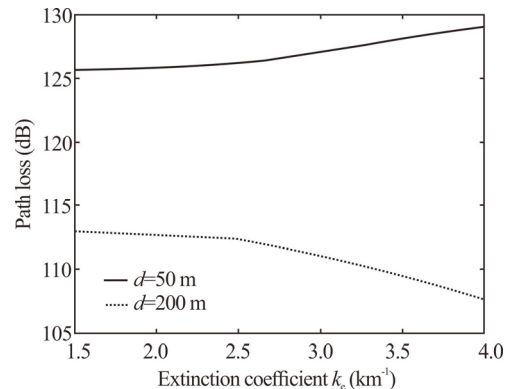


**Fig.5 Path losses for different aerosol extinction coefficients**

The path losses of water-soluble and the non-water-soluble polydisperse aerosol systems are demonstrated in Fig.7 and Fig.8. We vary the atmosphere visibility by changing the particle densities of water-soluble and the non-water-soluble aerosols. We have

calculated the path losses for two different particle densities, by assuming  $C=1, 2$  in Eq.(2). As shown in Tab.3, for  $C=1$ , the water-soluble aerosol system has the visibility of 111.8 km. For  $C=2$ , the water-soluble aerosol system has the visibility of 55.9 km. For  $C=1$ , the non-water-soluble aerosol system has the visibility of 2 km. For  $C=2$ , the non-water-soluble aerosol system has the visibility of 1 km.

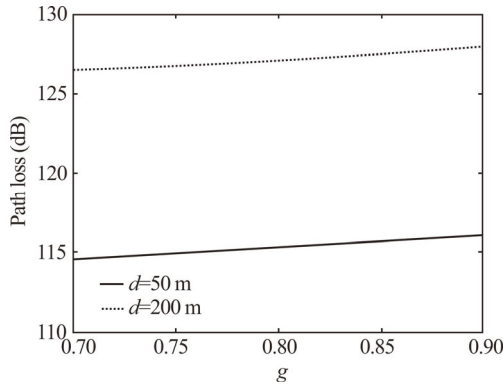


**Fig.6 Path losses for different asymmetry factors**

It is seen in Fig.7 and Fig.8 that within a short range the path loss is relatively low for low visibility weather, indicating the good performance of the communications for bad weather, which is a good situation for free-space communications. However, this good situation will not remain. The turning point occurs around  $d=90$  m for water-soluble aerosol, shown in Fig.7, and around  $d=150$  m for non-water-soluble aerosol, shown in Fig.8. Comparing Fig.7(a) and (b), we find the turning point is not sensitive to the elevation of the transmitter and the receiver. However, it is noted that the path losses for  $\theta_T=\theta_R=60^\circ$  are smaller than those for  $\theta_T=\theta_R=30^\circ$ . This is reasonable since for  $\theta_T=\theta_R=60^\circ$  the system geometry is more similar to the case of the LOS communication. We confirm the statements when comparing Fig.8(a) and (b) for the non-water-soluble aerosol. However, as seen in Fig.8, we note that for non-water-soluble aerosol, the path losses do not have that big difference for the low-visibility and large-visibility weathers. Furthermore, the path losses are not that sensitive to the elevation of the transmitter and the receiver. This can be explained by the fact that the non-water-soluble aerosol causes much smaller visibility than the water-soluble aerosol. It is expected that the performance of the communication system cannot be improved any more for specific low-visibility weather, which gives the lower limit of the path loss of the communication channel.

Additionally, comparing Fig.7 and Fig.8, for the same system geometry, the path losses are smaller for the water-soluble aerosol than the non-water-soluble aerosol, while water-soluble aerosol gives high-visibility weather, which seems to violate previous conclusions. Remember that the water-soluble aerosol has the normalized asymmetry factor of 0.70, which is much smaller than that of the non-water-soluble aerosol 0.88, shown in Tab.3. The

small  $g$  of water-soluble aerosol indicates the water-soluble aerosol scatters more light to the side than non-water-soluble aerosol. Scattering more light to the side with respect to the LOS direction means the receiver of the NLOS UV communication system captures more scattered light. Also note that the water-soluble aerosol has  $k_s/k_e=0.98$ , which is larger than  $k_s/k_e=0.69$  of non-water-soluble aerosol. This leads to the higher probability of the photons being scattered by the water-soluble aerosol. The above two factors result in the low path losses of the communication for water-soluble aerosol.

The above statements are further confirmed by the simulated path losses in the actual polydisperse aerosol systems, shown in Fig.9, where the measured visibilities of the four days are used. Due to the similar values of  $g$ , the path loss has direct relation with the visibility. It is clearly seen in Fig.9 that within limited communication range, i.e., around  $d<150$  m, the path loss increases with the visibility. The path losses of the communication channel for  $\theta_T=\theta_R=60^\circ$  are smaller than those for  $\theta_T=\theta_R=30^\circ$ . This situation is similar to the situation of the water-soluble and non-water-soluble polydisperse aerosol systems. We conclude that for actual polydisperse aerosol systems of low-visibility weather, within a short time interval, the similar atmosphere conditions lead to similar asymmetry factors. The path loss of the NLOS UV communication channel is hence exclusively determined by the atmosphere visibility.

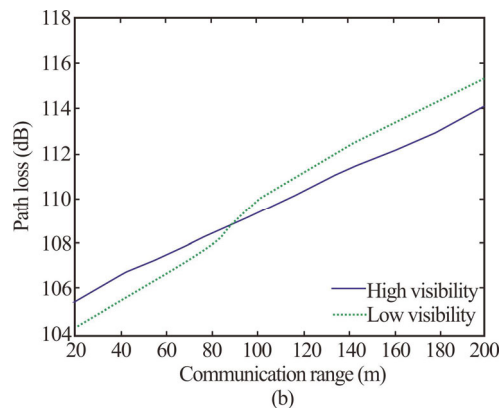
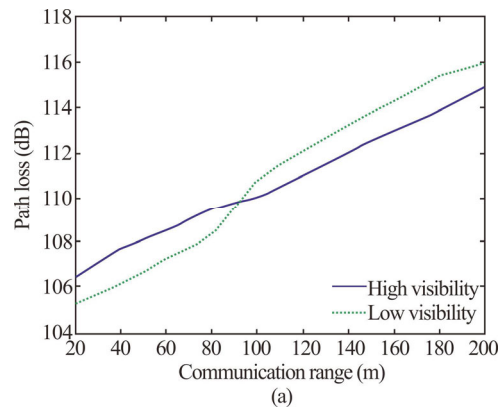


**Fig.7 Path losses of water-soluble aerosol for (a)  $\theta_T=\theta_R=30^\circ$  and (b)  $\theta_T=\theta_R=60^\circ$**

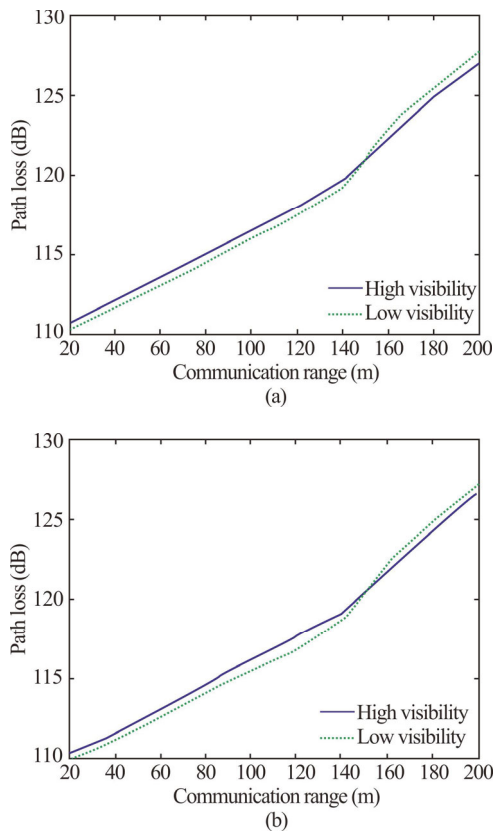


**Fig.8** Path losses of non-water-soluble aerosol for (a)  $\theta_T=\theta_R=30^\circ$  and (b)  $\theta_T=\theta_R=60^\circ$

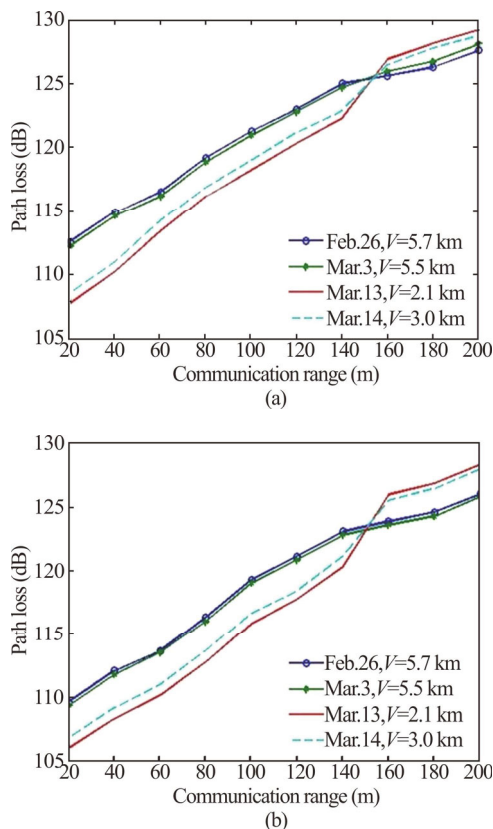


**Fig.9** Path losses of the actual aerosol for (a)  $\theta_T=\theta_R=30^\circ$  and (b)  $\theta_T=\theta_R=60^\circ$

In this paper, we performed a full analysis of the path losses of the NLOS UV communication channels with respect to the system geometry, communication range, and the atmospheric parameters, considering polydisperse aerosol system as the transmission media. Two polydisperse aerosol systems were used, aerosols with lognormal particle size distributions and the actual aerosols. A relation between the path loss of NLOS UV communication channel and the atmosphere visibility was presented. Simulation results show that for a limited communication range the path loss increases with the visibility. For longer communication range, the path loss will increase first and then decrease with the visibility. In most cases the position of turning point is determined by aerosol component and the atmosphere visibility level. It is also found that decreasing elevation of the transceiver may reduce the path loss, which can be expected since that NLOS communication with low elevation is similar to LOS communication. For the actual atmosphere, the atmosphere conditions can be similar within a short time interval. The path loss is hence exclusively determined by the atmosphere visibility.

Further research can be focused on the performance of the NLOS UV communication system under different atmosphere conditions. More spatial aerosol characteristics can be obtained in AERONET, or from the weather satellite, providing useful information for predicting the performance of the NLOS UV communication system.

**Statements and Declarations**

The authors declare that there are no conflicts of interest related to this article.

**References**

- [1] DING H S, LEI Y, YUAN Z L, et al. Fabrication and characteristics of ZnO nanoparticles ultraviolet photodetector[J]. Journal of optoelectronics·laser, 2018, 29(10): 1058-1063. (in Chinese)
- [2] SU B, LIU M, YAN Y S, et al. Effects of cathode buffer layers on the performance of organic ultraviolet photodetector based on m-MTDATA/BAIq[J]. Journal of optoelectronics·laser, 2015, 26(7): 1238-1242. (in Chinese)
- [3] YANG G, LI X Y, CHEN M, et al. A new neighbor discovery algorithm of TDMA in UV ad hoc network[J]. Journal of optoelectronics·laser, 2015, 26(6): 1074-1080. (in Chinese)
- [4] KE X Z, HE H, CHEN X. A new backoff algorithm of MAC layer in UV adhoc communication network[J]. Journal of optoelectronics·laser, 2010, 21(7): 1002-1006. (in Chinese)
- [5] XU Z, DING H, SADLER B M, et al. Analytical performance study of solar blind non-line-of-sight ultraviolet short-range communication links[J]. Optics letters, 2008, 33(16): 1860-1862.
- [6] XU Z. Approximate performance analysis of wireless

- ultraviolet links[C]//IEEE International Conference on Acoustics, Speech and Signal Processing, April 15-20, 2007, Honolulu, HI, USA. New York: IEEE, 2007, 3: 577-580.
- [7] GARG K K, SINGYA P, BHATIA V. Performance analysis of NLOS ultraviolet communications with correlated branches over turbulent channels[J]. *Journal of optical communications and networking*, 2019, 11(11): 525-535.
- [8] SONG P, LIU C, ZHAO T, et al. Research on pulse response characteristics of wireless ultraviolet communication in mobile scene[J]. *Optics express*, 2019, 27(8): 10670-10683.
- [9] CAO T, GAO X, WU T, et al. Single-scatter path loss model of LED-based non-line-of-sight ultraviolet communications[J]. *Optics letters*, 46(16): 4013-4016.
- [10] DING H, CHEN G, MAJUMDAR A K, et al. Modeling of non-line-of-sight ultraviolet scattering channels for communication[J]. *IEEE journal on selected areas in communication*, 2009, 27(9): 1535-1544.
- [11] XU C, ZHANG H. Channel analyses over wide optical spectra for long-range scattering communication[J]. *IEEE communications letters*, 2015, 19(2): 187-190.
- [12] ZHANG H, YIN H, JIA H, et al. Characteristics of non-line-of-sight polarization ultraviolet communication channels[J]. *Applied optics*, 2012, 51(35): 8366-8372.
- [13] DROST R J, MOORE T J, SADLER B M. UV communications channel modeling incorporating multiple scattering interactions[J]. *Journal of optical society America A optics image science & version*, 2011, 28(4): 686-695.
- [14] XU C, ZHANG H, CHENG J. Effects of haze particles and fog droplets on NLOS ultraviolet communication channels[J]. *Optics express*, 2015, 23(18): 23259-23269.
- [15] DING H, XU Z, SADLER B M. A path loss model for non-line-of-sight ultraviolet multiple scattering channels[J]. *EURASIP journal on wireless communications & networking*, 2010, 2010(1): 1-12.
- [16] LIN Y, XU Z, WANG J, et al. Analysis of effect of multiple scattering on non-line-of-sight scattering communication in fog weather[J]. *Acta photonica sinica*, 2014, 43(S1): 225-228.
- [17] DROST R J, MOORE T J, SADLER B M. Monte-Carlo-based multiple-scattering channel modeling for non-line-of-sight ultraviolet communications[J]. *Proceedings of SPIE-the international society for optical engineering*, 2011, 8038(5): 73-81.
- [18] LUO P, ZHANG M, HAN D, et al. Performance analysis of short-range NLOS UV communication system using Monte Carlo simulation based on measured channel parameters[J]. *Optics express*, 2012, 20(21): 23489-23501.
- [19] JIA H, CHANG S, YANG J, et al. Monte-Carlo simulation of atmospheric transmission characteristics in non-line-of-sight ultraviolet communication[J]. *Acta photonica sinica*, 2007, 36(5): 955-960.
- [20] HESS M, KOEPKE P, SCHULT I. Optical properties of aerosol and clouds: the software package OPAC[J]. *Bulletin of the American meteorological society*, 1998, 79(5): 831-844.
- [21] Aerosol robotic network[EB/OL]. <https://aeronet.gsfc.nasa.gov>.